Hydrometallurgy 109 (2011) 168–174

Contents lists available at ScienceDirect

Hydrometallurgy

journal homepage: www.elsevier.com/locate/hydromet

The sizing of oxygen bubbles in copper electrowinning

Reza Al Shakarji [a,1], Yinghe He [a,*], Simon Gregory [b,2]

[a] School of Engineering and Physical Sciences, James Cook University, QLD 4811, Townsville, Australia
[b] Xstrata Technology, Copper Refinery Limited, Hunter St, QLD 4811, Townsville, Australia

ARTICLE INFO

Article history:
Received 12 May 2011
Received in revised form 29 June 2011
Accepted 29 June 2011
Available online 12 July 2011

Keywords:
Copper electrowinning
Oxygen evolution
Imaging
Bubble size
Contact angle
Surface tension

ABSTRACT

Oxygen bubbles are formed on the anode in the copper electrowinning process. Burst of the bubbles produces acid mist in the tankhouse. While it is well acknowledged that the amount of acid mist is related to the size of the bubble, no systematic measurements have been made to quantify bubble size and its relationship with materials and process variables. This paper presents results of bubble size measurement under different operating conditions. For each of the operating conditions tested, bubbles were detected in a wide size distribution ranging from 20 μm to more than 400 μm in diameter. Statistical analyses on the measurement results showed that addition of FC-1100, a surfactant widely used in copper electrowinning to suppress acid mist, and solution temperature were the two most influential test parameters on the bubble size followed by the age of the anode. In contrast, current density and solution acidity had negligible effect.

1. Introduction

Electrowinning is an electrochemical process that is used to extract and refine metals such as Cu, Zn, Ni, Mn and Cd from their solutions. In most cases, the solution is acidic and oxidation of water molecules at the anode is the common counter reaction which results in the liberation of oxygen bubbles:

$$2H_2O_{(l)} \rightarrow O_{2(g)} + 4H^+_{(aq)} + 4e^- \quad (1)$$

The generation of oxygen bubbles generally requires a high overpotential and accounts for a considerable percentage of the energy consumption in metal electrowinning tankhouses. Moreover, the generated oxygen bubbles burst at the air/solution interface, producing highly acidic droplets of which the fine ones become airborne and form an acid mist throughout the tankhouse of the electrowinning plant.

Acid mist is highly corrosive and results in the corrosion of cathode plates, anode hanger bars, tankhouse equipment and building structures. It also poses a serious health hazard and causes extreme discomfort to the skin, eyes and respiratory systems of tankhouse workers. The effects of different process parameters on the amount of acid mist have been discussed in detail in our earlier publication (Al Shakarji et al., 2011).

Previous research results suggest that the amount of acid mist being generated is related to the size of the bursting bubbles (Liow et al., 2007). For electrowinning processes, although it is known that some operating parameters such as solution temperature can influence the size of the bubbles, there have been no systematic studies to quantify the effect of operating parameters on the size and size distribution of bubbles.

This paper reports results of bubble size measurement under different operating conditions. It also examines, quantitatively, the relationship between the median bubble size and five operating parameters in copper electrowinning. These parameters are anode age, electrical current density, solution temperature, sulphuric acid concentration of the solution, and the presence of a typical chemical mist suppressant such as FC-1100.

2. Experimental

2.1. Equipment setup

The copper electrowinning process was replicated in a bench-scale tank (EW cell). The equipment used in this investigation and its arrangements are shown in Fig. 1.

A peristaltic pump and four submersible heaters were used to maintain consistency in the composition and temperature of the solution for the duration of each test. To replicate industrial operations Pb–Ca–Sn alloy and 316 L stainless steel were used as anode and cathode, respectively (Houlachi et al., 2007). Areas of 100 mm wide and 150 mm long of the sides of electrodes facing each other were exposed to the solution and the rest of the immersed electrodes were isolated from the solution. This arrangement allowed

* Corresponding author. Tel.: +61 7 47814270; fax: +61 7 47816788.
E-mail addresses: reza.alshakarji@my.jcu.edu.au (R. Al Shakarji), yinghe.he@jcu.edu.au (Y. He), sgregory@xstratatech.com (S. Gregory).
[1] Tel.: +61 422347562; fax: +61 7 47816788.
[2] Tel.: +61 7 47589530; fax: +61 7 47589501.

0304-386X/$ – see front matter © 2011 Elsevier B.V. All rights reserved.
doi:10.1016/j.hydromet.2011.06.010

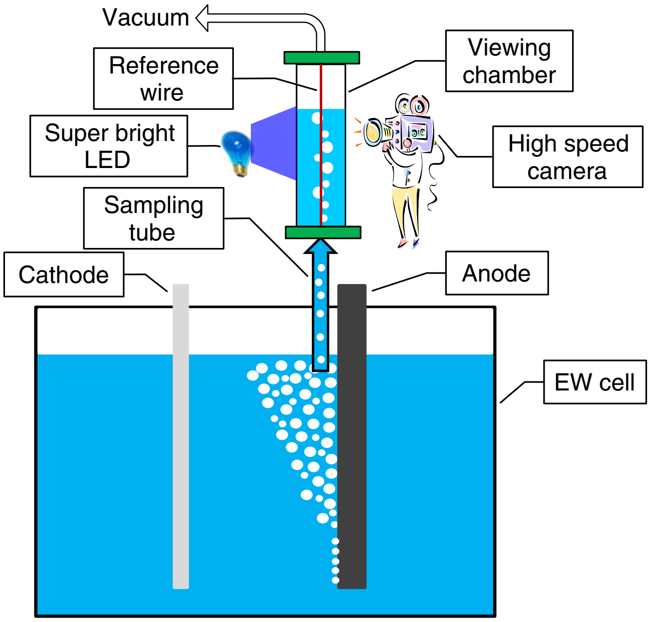

Fig. 1. A schematic view of equipment setup (not to scale).

a precise and controlled electrical current flow through the solution via the specified electrodes surfaces.

For each set of experiments a fresh batch of solution was synthesized containing 45 g L^{-1} Cu, 15 mg L^{-1} Guar gum, 20 ppm Cl, 100 ppm Co, and various amounts of sulphuric acid. The concentration of Cu, Guar gum, Cl and Co in the synthesized solution was similar to the electrolyte solutions found in most copper electrowinning tankhouses worldwide (Robinson et al., 1994). The sulphuric acid concentration in the solution, however, was one of the five selected variables and its concentration differed from that of a typical copper electrolyte solution.

To measure bubble sizes via image analysis, the generated oxygen bubbles were transferred from the EW cell to a viewing chamber. A high-speed camera (RedLake MotionXtra HG-100K) with a special macro lens and super bright blue LEDs were utilized to capture images of the rising bubbles in the viewing chamber.

2.2. Experimental design

The main goal of the present work was to compare, quantitatively, the effect of different operating parameters on bubbles sizes during a typical copper electrowinning process. To fully explore the main effect of each individual parameter as well as any possible interaction effects, the 2 K factorial method was used to determine the number of required experimental conditions (Montgomery, 2005). Based on this method, the test parameters were examined at two levels (low and high). Table 1 lists the five selected parameters and their low and high level values.

The values shown in Table 1 were selected so that the midpoint between low and high levels of each parameter represented the typical value used in most copper electrowinning tankhouses (Houlachi et al., 2007). For example, a sulphuric acid concentration in the electrolyte solution of about 170 g L^{-1} is typically used in most copper electrowinning operations. Thus, the low and high limits of solution acidity for the experiments were set at 100 and 250 g L^{-1}, respectively.

Based on the 2 K factorial method, 32 parameter combinations were required to fully examine the effect of five parameters at two levels. For reliable data analysis, a minimum of two replicates were required for each test condition. Hence, 64 tests were conducted to determine the significance of each parameter and also to identify any significant interactions among the selected parameters.

For each of the 64 experiments, at least two sets of high resolution photos were taken by the high-speed camera. The images were taken at 10 min intervals at a rate of 250 frames per second while the experiment was being conducted. To ensure that the same bubbles were not accounted for more than once, only one photo was selected per 100 consecutive frames (i.e. 3 to 5 photos were selected from each set of images of each experiment) for image analysis.

Table 1
The selected test variables and their values.

No	Examined parameter	Low	High
1	Anode age (months)	0	6
2	Current density (A m^{-2})	200	400
3	Temperature (°C)	30	60
4	Acidity (g L^{-1})	100	250
5	FC-1100 (ppm)	0	30

2.3. Bubble sizing process

A flexible silicon tube (sampling tube in Fig. 1) was used to transfer the bubble-containing solution from the EW cell to the viewing chamber. One end of the sampling tube was placed about 10 mm underneath the free surface of solution near the surface of the anode while the other end was connected to the bottom of the viewing chamber. By applying a gentle vacuum to the viewing chamber, the bubble containing solution was drawn from the EW cell to the viewing chamber at low flow rates. The large internal diameter of the sampling tube (5 mm) and the low solution flow rate, from the EW cell to the viewing chamber, ensured no bubble breakage or coalescence occurred during the bubble transfer process. Thus, bubbles observed in the viewing chamber were true representatives of those generated in the EW cell.

The high speed camera was then used to capture 800 × 600 pixel images. Each image taken from the rising bubbles in the viewing chamber contained about 100 bubbles on average (more than 300 bubbles in some cases). A MATLAB based program was developed to automate the analyses of the captured images. The developed program was able to process the images in grey scale format directly from the camera. The software was designed to take into account the uneven background illumination and to distinguish the boundaries of each bubble from its surroundings.

A thin copper wire, 130 μm in diameter, was fixed inside the viewing chamber adjacent to the solution's entrance. The diameter of this wire was used as a reference to determine the size of the bubbles captured in each image. The developed software was able to process each image in a few seconds and export the raw data of bubble diameters (in μm) to an Excel file. The software also indicated the detected bubbles with blue lines along the boundaries of each bubble and displayed the bubble diameter (in μm) next to it (Fig. 2). These processed images were used to visually inspect the results of the bubble sizing process.

To ensure the accuracy of the developed bubble sizing program, ImageJ (an open source image analysis software) was used to manually determine the bubble sizes of three randomly selected images. The results of the automated and manual bubble sizing were statistically identical.

3. Results and discussion

3.1. Overall statistical analysis

In total, more than 54,000 bubbles were sampled and their sizes measured. The diameter of the bubbles ranged predominantly from 26 μm up to 182 μm, on average, for each of the 64 experiments.

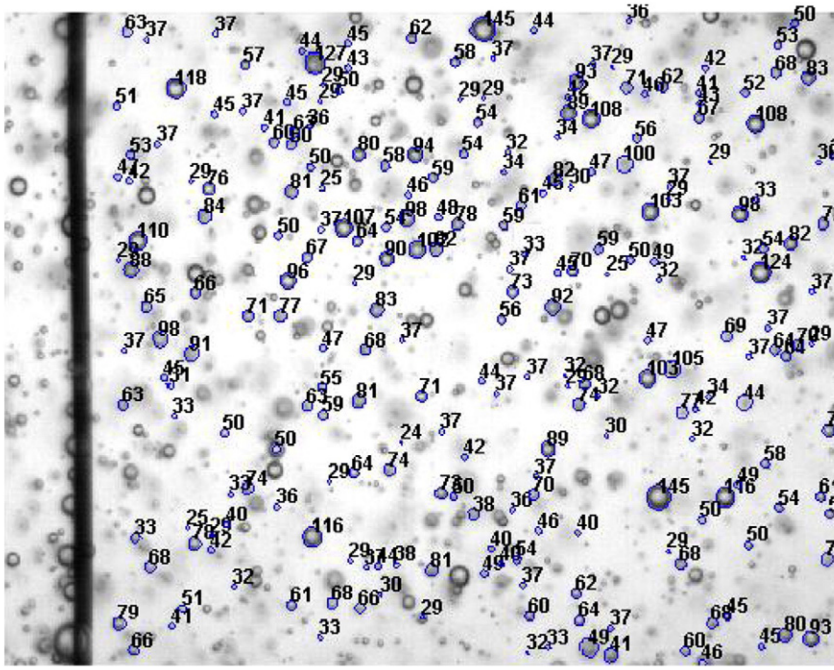

Fig. 2. A processed image with 250 detected bubbles and the reference wire (the vertical black line) appearing on the far left.

However, there were cases where the smallest detected bubble was 20 μm and the largest one was 404 μm. On average, 50% of the detected bubbles had a diameter of 53 μm or less (i.e. the grand median value). A typical bubble size distribution and cumulative percentage graph is shown in Fig. 3.

There was a relatively strong positive skewness (1.7 on average) in all the collected data samples, similar to that shown in Fig. 3. Therefore, median values were selected instead of mean values to represent the average bubble size for each experiment. The small difference between the medians of replicates of a test condition, which ranged from 0.00 μm up to 5.24 μm with the average being 2.17 μm, was a good indication of the high repeatability of the conducted experiments.

Fig. 4 illustrates the median bubble diameter (the bold black line inside each box), the lower and upper quartiles (the lower and upper edges of each box), the lower and upper extremes (the lower and upper whiskers), and also the outliers (the stars) for each of the 32 experimental conditions. The values of median bubble diameters ranged from 43 μm to 66 μm. Regardless of the applied operating conditions, 95% of the generated bubbles were less than 106 μm in

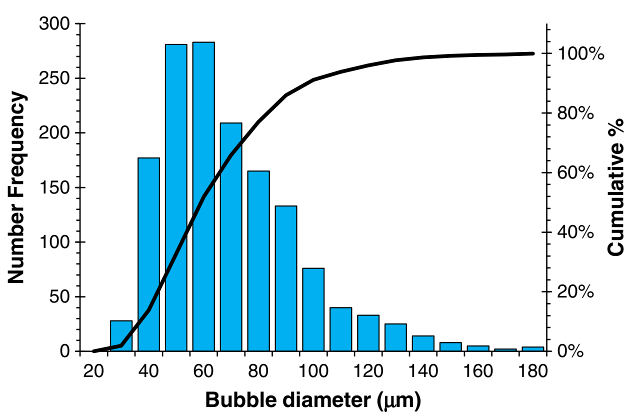

Fig. 3. Bubble size distribution and cumulative percentage graph for experiment No 9 (parameter values: new anode, 200 A m^{-2} current density, 60 °C solution, no FC-1100 and 100 g L^{-1} sulphuric acid concentration).

diameter. It must be noted that the outliers were neither the result of error in the bubble sampling process nor the image analysis procedure. Live video footage taken from the surface of an immersed operating anode proved the existence of such unusually large bubbles. More details about these outliers can be found in our previous publication (Al Shakarji et al., 2010).

A 5-way ANOVA analysis was performed on the raw experimental data to determine the full effect of test parameters on the average bubble size. To quantify the magnitude of the effect of each of the 32 parameter combinations, Pearson's r value was calculated for each case based on its ANOVA's mean square value (Field, 2005). Cohen classifies the magnitude of a parameter's effect into three categories of small, medium and large (Cohen, 1988). These categories correspond to Pearson's r values of 0.1, 0.3 and 0.5 respectively (Cohen, 1988). Parameter combinations with Pearson's r value greater than 0.10 are shown in Fig. 5.

FC-1100 and solution temperature, having the highest r values in Fig. 5, were the most influential parameters in determining the final bubble sizes. To a lesser extent, anode age also influenced the final bubble sizes. Current density and solution acidity, with Pearson's r values of 0.04 and 0.05 respectively (not shown in Fig. 5), had negligible effect on the detachment size of bubbles.

The full factorial ANOVA analysis not only examined the effect of individual parameters but also all the possible parameter interactions. This analysis returned an R^2 value of 0.951, which meant the variations made in the test parameters of the conducted experiments could explain more than 95% of the bubble size variations measured in the test series.

3.2. Effect of individual parameters on bubble size

To assess the effect of individual test parameters on the bubble size, the average median bubble diameter for each level of a parameter was calculated. Each bar in Fig. 6 represents the averaged median bubble diameter from 32 independent experiments.

3.2.1. FC-1100

FC-1100 was the only parameter that had a large effect, based on Cohen's classification, on the average bubble sizes. The presence of FC-

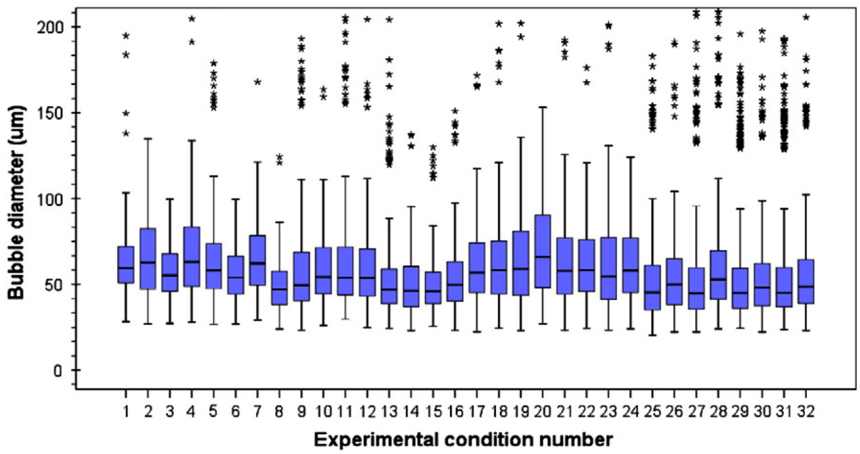

Fig. 4. Bubble size distribution under 32 different operating conditions.

1100 in the solution reduced the average bubble diameter by 9.3 μm. This result was largely attributed to the ability of FC-1100 to reduce the surface tension of the electrolyte from 63 mN m^{-1} to 44 mN m^{-1}. The near parallel solid lines in Fig. 7 implied that, within the tested range, the effectiveness of FC-1100 in reducing the final bubble sizes was independent of the solution temperature.

The bubble size distribution, in addition to the average bubble size, was also considerably reduced in the presence of FC-1100 (Fig. 8). It was proposed that the presence of FC-1100 molecules reduced the surface tension of the solution to a degree that resulted in less variation in the three phase contact angle on the anode, leading to the generation of more uniformly sized bubbles (i.e. smaller standard deviation).

3.2.2. Temperature

Solution temperature with a Pearson's r value of 0.30 was the second most influential parameter in determining the final size of a bubble (Fig. 5). Changing the solution temperature caused a relatively large difference in the average bubble diameter. Raising the temperature of the solution from 30 °C to 60 °C resulted in 3.7 μm reduction in the average bubble sizes, equivalent to 0.150 standard deviations (Fig. 6).

Similar to the presence of FC-1100, when temperature of the solution was raised from 30 °C to 60 °C, surface tension of the electrolyte solution decreased from 63 mN m^{-1} to 44 mN m^{-1}. Therefore, it was postulated that the decrease in the average bubble size at higher temperature was mainly due to the decrease in the surface tension of the solution. The large reduction in surface tension

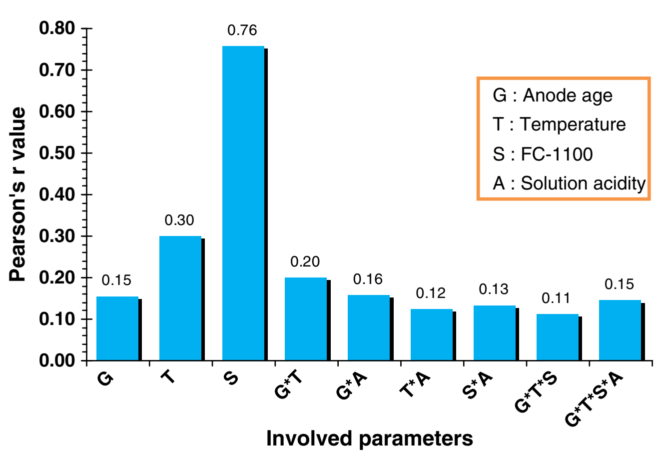

Fig. 5. Quantitative comparison of the most influential parameters and parameter interactions on the average bubble size.

due to temperature rise was also expected to result in less variation in the three phase contact angle, leading to the generation of more uniformly sized bubbles. This expectation was confirmed by data presented in Fig. 9 where bubble size distribution was noticeably less (smaller box and whiskers) in high temperature electrolyte solution.

3.2.3. Anode age

The experimental results shown in Fig. 6 suggested that bubbles generated on an old anode were, on average, 2.0 μm (0.089 standard deviations) larger than those generated on a new anode. The ANOVA analysis resulted in a Pearson's r value of 0.15 for the anode age which meant this parameter had a small/medium effect on the final size of a bubble. It was postulated that anode age affected the detachment size of a bubble by influencing the liquid–solid–gas contact angle which in turn influenced the balance of the forces acted on the bubble. SEM images revealed that the surface of an old anode was highly uneven and covered with voids and micro cracks whereas the surface of a new anode was relatively smooth and even (Fig. 10).

It was likely that the small cavities and cracks on the surface of the old anode provided much higher number of nucleation sites for the bubbles, leading to “forced” coalescence of the bubbles during their growth on the anode immediately prior to their detachment due to insufficient distances between neighbouring bubbles on the anode. Similar observations were reported by Huet where mean detachment radius of electrolytic bubbles increased with the surface roughness of nickel electrodes (Huet et al., 2004).

It is important to note that, regardless of the age of the anodes or operating conditions, bubble size distribution was relatively large, ranging from 20 μm to more than 400 μm (Fig. 4). The heterogeneities in both the chemical composition and the surface roughness of the anodes were believed to be the main reasons for such wide bubble size distributions. The anodes were Pb–Ca–Sn cold rolled alloys, either the surface roughness or the distribution of the three elements was very unlikely to be even on the surface of the anodes after the rolling process.

3.2.4. Solution acidity and current density

It is worth noting that, within the ranges tested in this study, both the solution acidity and the current density had negligible influence on the bubble size. Solution acidity could affect the bubble size only through the change it could cause in the solution viscosity. Kazakis et al. reported a noticeable difference in the average bubble size only when the viscosities of the test solutions were considerably different, e.g. the difference between their viscosities was more than 600% (Kazakis et al., 2008). Rheological tests of the copper electrolyte solutions, however, showed that high acidity solutions were only 21% more viscous than low acidity solutions. Therefore, it was suggested

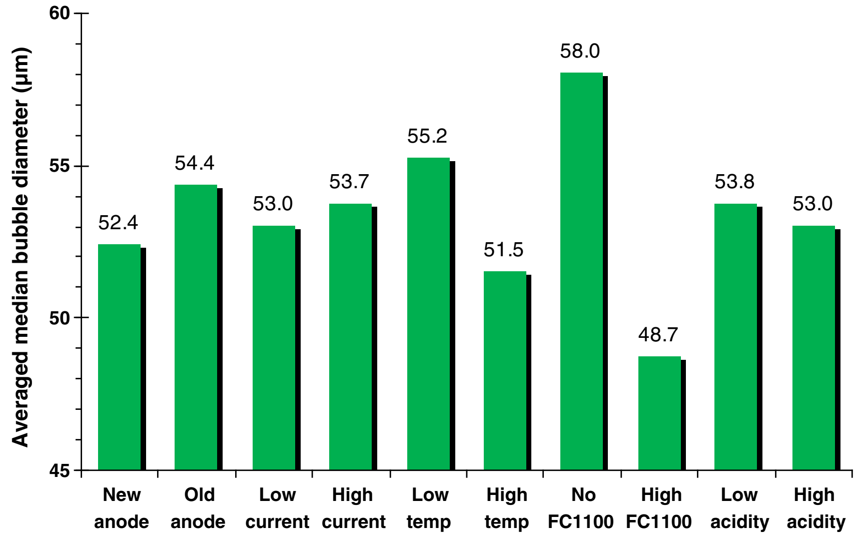

Fig. 6. Average bubble diameter at different operating conditions.

that a much larger difference in the solution acidity, and hence the viscosity, was required to observe a noticeable difference in the average size of the bubbles generated during the copper electrowinning process.

Based on Faraday's law, increasing the electrical current density would increase the amount of oxygen produced at the anode (Harris, 2007). Consistent with our results presented previously, within the range of 200 and 400 $A m^{-2}$, a change in the current density had caused only a change in the bubble nucleation rate and hence the number of bubbles generated per unit time. The final size of the bubbles changed little with current density (Al Shakarji et al., 2010).

3.3. Effect of parameters' interaction on bubble size

Few publications in this field studied the interactions that exist among the test parameters. The full factorial ANOVA analysis showed that more than 22% of variations in bubble sizes recorded in the test series were due to the interactions between the test parameters.

With a Pearson's r value of 0.20, the anode age–temperature interaction (G*T) was identified as the most significant parameter interaction. The results are shown in Fig. 11.

It can be seen that, on an old anode, increasing the temperature of the solution from 30 °C to 60 °C resulted in a relatively large decrease (more than 0.247 standard deviations) in the average bubble diameter. In contrast, the same increase in the solution temperature resulted in a much smaller decrease (about 0.049 standard deviations) in the average bubble diameter on a new anode.

The G*T interaction not only affected the average size but also the size distribution of bubbles. Size distribution of bubbles formed on the old anode was much wider at low solution temperature in comparison to that of high solution temperature (i.e. larger box and whiskers at low solution temperature). In contrast, the temperature of the solution had a relatively small effect on the size distribution of bubbles formed on a new anode (i.e. similar box and whiskers sizes at low and high temperatures).

The decrease in the average bubble size and its distribution with temperature rise was due to surface tension reduction as explained earlier. Consistent with observations made by other researchers (Drelich and Miller, 1994; Meiron et al., 2004), the strong interaction between anode age and solution temperature was believed to be mainly due to the effect of anode's surface morphology on the three phase contact angle.

The effect of the anode's surface morphology (i.e. anode age) on bubble size and its distribution was much more evident at low solution temperature (Fig. 11) since the overall surface tension was higher at lower temperature.

One of the other important interactions was the T*A interaction. The decrease in the average bubble size and its distribution due to temperature rise was not the same for the low and high acidity solutions (Fig. 12). The average size and size distribution of bubbles were more strongly affected by temperature rise in low acidity solutions than in high acidity solutions.

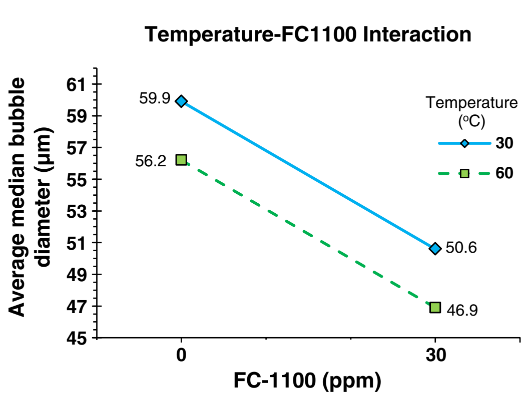

Fig. 7. The effect of FC-1100 on bubble size at different temperatures.

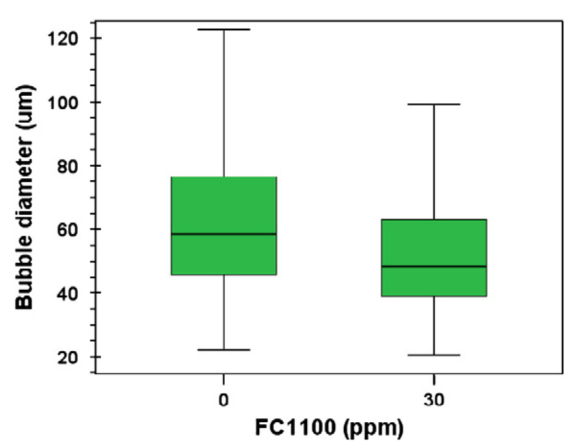

Fig. 8. Effect of FC-1100 on bubble size distribution (not including outliers).

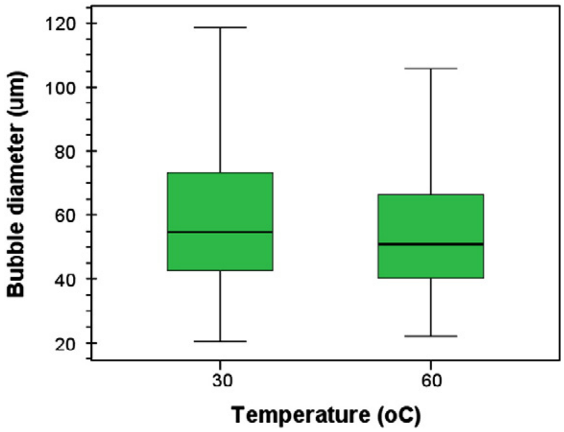

Fig. 9. Effect of solution temperature on bubble size distribution (not including outliers).

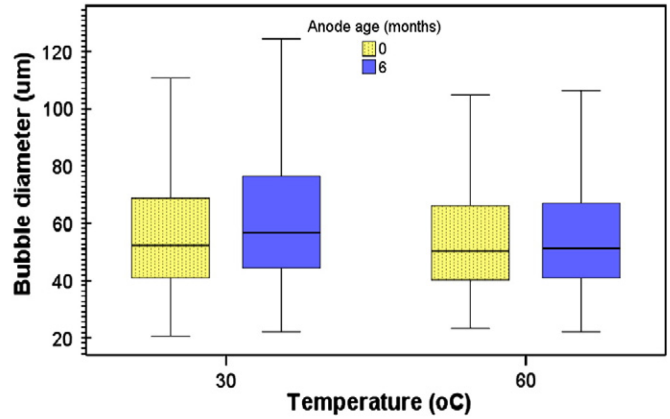

Fig. 11. The interaction between anode age and temperature.

Surface tension and viscosity were both known to influence the final size of a bubble (Xie et al., 2009; Xu et al., 2009). Temperature affected both surface tension and viscosity whereas acidity only affected viscosity. Therefore, the T*A interaction was expected to be the result of surface tension and viscosity interaction. The surface tensions of low and high acidity solutions were measured at two different temperatures (Fig. 13).

It is general knowledge that surface tension of a liquid is a function of not only its composition but also its temperature. Measurements showed that surface tension of a low acidity solution was higher than that of a high acidity solution at 30 °C (Fig. 13). However, surface tensions of the two solutions were almost the same at 60 °C. In other words, temperature had a more profound effect on the surface tension of low acidity solutions than that of high acidity solutions. These observations were similar to those seen in Fig. 12 in that, in low acidity solutions, the differences in the average bubble size and bubble size distribution caused by temperature rise were much larger. Both figures demonstrated a strong interaction between temperature and solution acidity.

The surfactant–solution acidity (S*A) interaction had a Pearson's r value of 0.13. The interaction between FC-1100 and solution acidity is illustrated in Fig. 14.

In the absence of FC-1100, although bubble size distribution was slightly larger in high acidity solutions, the average bubble sizes generated in the low and high acidity solutions were very similar. In the presence of FC-1100, bubbles generated in high acidity solutions were on average 0.101 standard deviations smaller in diameter than those generated in low acidity solutions. Xu et al. also reported similar observations when studying the effect of NaCl concentrations on bubbles generated from a sparger in the presence of fixed amounts of sodium dodecyl sulphate surfactant (Xu et al., 2009). The higher ionic concentration at high acidity solutions was speculated to result in closer packing of the surfactant molecules by reducing the repulsive forces between them (Xu et al., 2009). In our case, bulk concentration of FC-1100 in high acidity solutions might be lower, resulting in more FC-1100 molecules packing at the interface. This can be inferred from the fact that the average surface tension of low acidity solutions is higher than that of high acidity solutions. The closer packing of the surfactant molecules at the oxygen/solution interface lowers the surface tension and results in smaller bubbles.

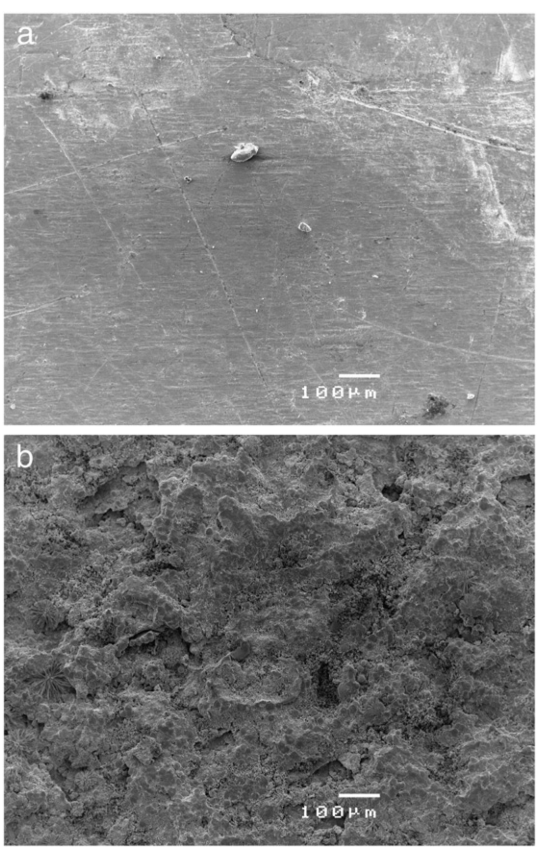

Fig. 10. The surface morphology of (a) a new anode (b) an old anode.

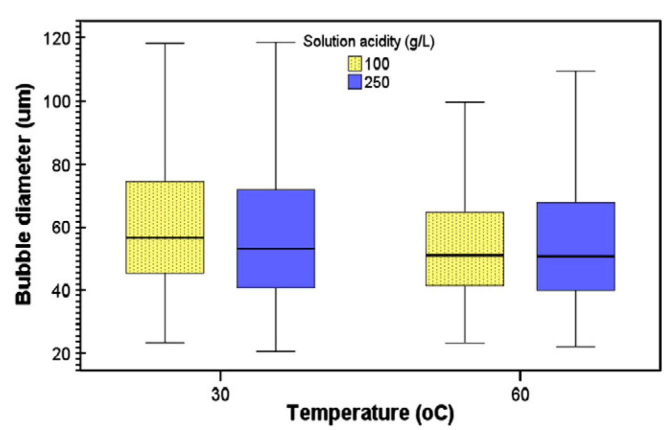

Fig. 12. The interaction between temperature and solution acidity.

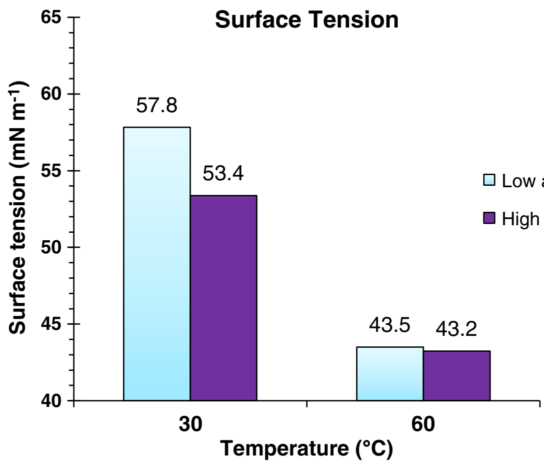

Fig. 13. Effect of temperature and acidity on surface tension.

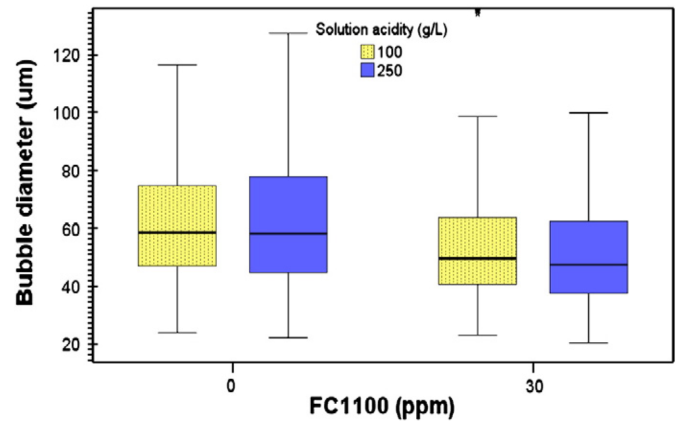

Fig. 14. The interaction between FC-1100 and solution acidity.

4. Conclusions

A high-speed camera and image analysis software were used to measure the size of the bubbles generated during the copper electrowinning process. Measurements, made under a variety of operating conditions, showed that of the five test parameters, FC-1100 and solution temperature had the most significant effect on the average size of the oxygen bubbles. Bubble size and bubble size distribution were noticeably reduced in the presence of FC-1100 or when the solution temperature was increased. FC-1100 and solution temperature both influenced bubble sizes by reducing the overall surface tension of the solution. To a lesser extent, anode age also influenced the detachment size of bubbles. Older anode generated larger bubbles and wider bubble size distributions mainly due to its surface roughness variations.

The data produced by the present work can be used to investigate the correlation between bubble size and the amount of acid mist, facilitating the design of strategies for minimizing acid mist generation in the tankhouse. The data can also be used to calculate the rate of bubble generation and release under a variety of operating conditions. Such information would be extremely useful in simulating the flow pattern of electrolyte solution between electrodes, which can be utilized to enhance the design of the electrodes and cells leading to improved electrolyte flow and copper quality at higher current densities.

Acknowledgment

The authors gratefully acknowledge the partial financial and technical support of Xstrata Technology. We also would like to thank Mr Tony Ruddell and Mr Curtis Arrowsmith who assisted us with the design and fabrication of the apparatus used in the test work.

References

Al Shakarji, R., He, Y., Gregory, S., 2010. Measurement of bubble size distribution in copper electrowinning process by image analysis. In: Harre, J. (Ed.), 7th International Copper Conference. GDMB, Hamburg Germany, pp. 1237–1251.
Al Shakarji, R., He, Y., Gregory, S., 2011. Statistical analysis of the effect of operating parameters on acid mist generation in copper electrowinning. Hydrometallurgy 106 (1–2), 113–118.
Cohen, J., 1988. Statistical Power Analysis for the Behavioural Science. Lawrence Erlbaum Associates Inc, New Jersey.
Drelich, J., Miller, J.D., 1994. The effect of solid surface heterogeneity and roughness on the contact angle/drop (bubble) size relationship. Journal of Colloid and Interface Science 164 (1), 252–259.
Field, A., 2005. Discovering Statistics Using SPSS. SAGE Publications Ltd., London.
Harris, D.C., 2007. Quantitative Chemical Analysis. Freeman and Co., New York.
Houlachi, G.E., Edeards, J.D., Robinson, T.G., 2007. Copper Electrorefining and Electrowinning, V. Canadian Institute of Mining, Metallurgy and Petroleum, Quebec Canada.
Huet, F., Musiani, M., Nogueira, R.P., 2004. Oxygen evolution on electrodes of different roughness: an electrochemical noise study. Journal of Solid State Electrochemistry 8 (10), 786–793.
Kazakis, N.A., Mouza, A.A., Paras, S.V., 2008. Experimental study of bubble formation at metal porous spargers: effect of liquid properties and sparger characteristics on the initial bubble size distribution. Chemical Engineering Journal 137 (2), 265–281.
Liow, J.L., Frazer, A., He, Y., Eastwood, K., Phan, C., 2007. Acid Mist Formation in the Electrowinning of Copper. Chemeca, Chemeca, Melbourne Australia.
Meiron, T.S., Marmur, A., Saguy, I.S., 2004. Contact angle measurement on rough surfaces. Journal of Colloid and Interface Science 274 (2), 637–644.
Montgomery, D.C., 2005. Design and Analysis of Experiments. John Wiley & Sons Inc, New York.
Robinson, T., Lang, J., Isbell, L., 1994. Cerro Colorado Copper Company SX-EW Plant. ISA PROCESS Tankhouse, Colorado USA.
Xie, G.X., Luo, J.B., Liu, S.H., Guo, D., Li, G., Zhang, C.H., 2009. Effect of liquid properties on the growth and motion characteristics of micro-bubbles induced by electric fields in confined liquid films. Journal of Physics D — Applied Physics 42 (11), 12.
Xu, Q., Nakajima, M., Ichikawa, S., Nakamura, N., Roy, P., Okadome, H., Shiina, T., 2009. Effects of surfactant and electrolyte concentrations on bubble formation and stabilization. Journal of Colloid and Interface Science 332 (1), 208–214.